Sequence-dependent trafficking of GDE2, a GPI-specific phospholipase promoting neuronal differentiation

Fernando Salgado-Polo,[1] Michiel van Veen,[2] Bram van den Broek,[2] Daniela Leyton-Puig,[2] Roy Baas,[1] Anastassis Perrakis,[1] Wouter H. Moolenaar,[1,*] and Elisa Matas-Rico[1,*]

[1]Division of Biochemistry, [2]Division of Cell Biology
The Netherlands Cancer Institute
Plesmanlaan 121, 1066 CX Amsterdam
The Netherlands

*Correspondence: w.moolenaar@nki.nl; e.matas@nki.nl

Summary

GDE2 is a six-transmembrane glycerophosphodiesterase with phospholipase D-like activity that cleaves select glycosylphosphatidylinositol (GPI)-anchored proteins and thereby influences biological signaling cascades. GDE2 promotes neuronal differentiation cell-autonomously through glypican cleavage and is a prognostic marker in neuroblastoma, while GDE2 deficiency causes progressive neurodegeneration in mice and developmental defects in zebrafish. However, the regulation of GDE2 remains unclear. Here we show that in undifferentiated neuronal cells, GDE2 undergoes constitutive internalization and traffics back along both fast and slow recycling routes, while a small percentage is sorted to late endosomes. GDE2 trafficking is dictated by distinctive C-terminal tail sequences that determine secretion, endocytosis and recycling preference, respectively, and thereby regulate GDE2 function both positively and negatively. Our study reveals the sequence determinants of GDE2 trafficking and surface localization, and provides insight into the control of GPI-anchored protein activities with potential implications for nervous system disorders associated with impaired trafficking and beyond.

Keywords: glycosylphosphatidylinositol, GPI-anchored protein, glycerophosphodiester phosphodiesterase, Rab GTPase, endocytosis, recycling, neuroblastoma, neurodegeneration

Introduction

The surface of eukaryotic cells contains a great variety of glycosylphosphatidylinositol (GPI)-anchored proteins, many of which are involved in the regulation of vital cellular functions, including receptor signaling, cell adhesion, differentiation and cell-cell communication. GPI-anchoring is a highly complex post-translational modification that tethers membrane proteins via their C-terminus to a unique glycosylated phosphatidylinositol (PI) core in the outer leaflet of the plasma membrane (Ferguson et al., 2015; Fujita and Kinoshita, 2010; Paulick and Bertozzi, 2008). Since they lack a transmembrane domain, GPI-anchored proteins cannot transmit signals by themselves but must interact with transmembrane effectors to achieve signaling competence. Importantly, GPI-anchoring confers a unique property to membrane proteins, namely susceptibility to phospholipase attack. Indeed, GPI-anchored proteins can be released from their anchor and detected as soluble proteins, some of which are considered disease biomarkers. Yet, identification of the responsible phospholipase(s) has long been elusive. A secreted GPI-specific phospholipase D (GPI-PLD) does not act on intact cells (Low and Huang, 1991), whereas a cell-associated GPI-PLD activity that releases GPI-anchored proteins has remained unidentified to date (Metz et al., 1994).

Recent studies have advanced the field by showing that members of the glycerophosphodiester phosphodiesterase (GDPD) family, notably GDE2 and GDE3, function as GPI-specific phospholipases that cleave select GPI-anchored proteins and thereby alter signaling cascades and cell behavior (Matas-Rico et al., 2016; Park et al., 2013; van Veen et al., 2017). GDE2 (or GDPD5) is the best studied family member and, along with GDE3 and GDE6, is characterized by six transmembrane domains, a catalytic GDPD ectodomain and intracellular N- and C-terminal tails (**Fig. 1A,B**). GDE2 acts in a phospholipase D (PLD)-like manner towards soluble substrates (*i.e.* releasing choline from glycerol-3-phosphocholine (Gallazzini et al., 2008)) in common with virtually all GDPD family members (Corda et al., 2014; Ohshima et al., 2015). One notable exception is GDE3 (GDPD2), which functions as a phospholipase C (PLC) showing substrate selectivity different from GDE2 (Corda et al., 2009; van Veen et al., 2017).

GDE2 was originally shown to drive neuronal differentiation and survival in the developing spinal cord through surface cleavage of GPI-anchored RECK, an ADAM metalloprotease inhibitor and Notch ligand regulator, leading to inhibition of Notch signaling and induction of differentiation in adjacent neural progenitors (Park et al., 2013). More recently, we reported that GDE2 promotes neuronal differentiation in a cell-autonomous manner through surface cleavage of Glypican 6 (GPC6), one of the six GPI-anchored heparan sulfate proteoglycans (Matas-Rico et al., 2016). Enforced GDE2 expression led to altered Rho/Rac signaling, induction of neural differentiation markers, cell spreading, neurite outgrowth and resistance to RhoA-driven neurite retraction

(Matas-Rico et al., 2016). Furthermore, GDE2 expression was found to strongly correlate with favorable outcome in neuroblastoma, a childhood malignancy characterized by impaired neuronal differentiation (Matas-Rico et al., 2016). In mice, *Gde2* knockout led to progressive neurodegeneration in the spinal cord with pathologies reflecting human neurodegenerative disorders, which was accompanied by reduced glypican shedding (Cave et al., 2017). Finally, depletion of GDE2 in zebrafish embryos led to impaired motility and reduced pancreas differentiation and insulin expression; the latter phenotype could be rescued by human GDE2, indicating conservation of human and zebrafish GDE2 function (van Veen et al., 2018). Altogether, these results underscore the need for tight control of GDE2 surface expression and activity *in vivo*. However, it is still unknown how GDE2 surface levels and function are regulated.

Here we report that in undifferentiated neuronal cells, GDE2 undergoes constitutive endocytosis and recycling along distinct Rab GTPase-regulated trafficking routes, while a small part is sorted to late endo-lysosomal compartments. Through progressive C-terminal truncations, we define distinctive sequences that govern GDE2 exocytosis, endocytosis and recycling pathway preference, respectively. We show that these sequences regulate GDE2 surface expression and function, both positively and negatively, as measured by GPC6 shedding and induction of neural differentiation markers. Our study establishes a link between endocytic recycling and GDE2 function in neuronal cells, of potential relevance for nervous system disorders associated with impaired membrane trafficking.

Results

GDE2 localization and trafficking: predominance in recycling endosomes

We selected undifferentiated neuronal cells that express very low levels of endogenous GDE2, namely SH-SY5Y and N1E-115 cells (Matas-Rico et al., 2016). In these cells, GDE2 (GFP-, mCherry- or HA-tagged) is detected in discrete microdomains, or clustered nanodomains (rafts), as shown by super-resolution microscopy (Matas-Rico et al., 2016) (**Fig. 1C).** In addition, GDE2 is abundant in endocytic vesicles, particularly in the perinuclear region (**Fig. 1C)** (Matas-Rico et al., 2016). Treatment of the cells with the dynamin inhibitor dynasore resulted in GDE2 accumulation at the plasma membrane with almost complete loss of GDE2-positive vesicles, indicating that GDE2 undergoes dynamin-dependent internalization instead of bulk endocytosis (**Fig. S1A**). GDE2-GFP-containing vesicles are highly mobile and show rapid directional movement towards the tips of developing neurites, as shown by fluorescence live-imaging (**Movie S1**).

Rab GTPases are master regulators of membrane trafficking and show high selectivity for distinct endosomal compartments (Hutagalung and Novick, 2011; Wandinger-Ness and Zerial, 2014). To determine the nature of the GDE2-containing vesicles, we used Rab GTPase markers of early, late and recycling endosomes, respectively. In both neuronal cell lines, GDE2-GFP co-localized with early endosome marker Rab5-mCh (**Fig.1D** and **Fig. S1B**)**.** Rab5 coordinates clathrin-mediated endocytosis and biogenesis of early endosomes and their fusion. The majority of intracellular GDE2 was detected in two distinct populations of recycling endosomes, namely those representing the Rab4- and Rab11-dependent recycling routes ("fast" and "slow**",** respectively) (**Fig. 1D and S1B**). Rab4-dependent fast recycling of membrane cargo involves a half-time of a few minutes, whereas Rab11 regulates slow recycling through perinuclear endosomes with a half-time of about 12 minutes (Maxfield and McGraw, 2004). In addition, GDE2 was found to co-localize with the endogenous transferrin receptor (TrfR), a prototypic cargo in clathrin/dynamin-mediated recycling pathways (Mayle et al., 2012).

Finally, a relatively small fraction of GDE2 was detected in Rab7-positive ($Rab7^+$) late endosomes, also known as multi-vesicular bodies (MVBs), which deliver endocytosed cargo to lysosomes for proteolytic degradation (Langemeyer et al., 2018; Scott et al., 2014). Consistent with this, a small fraction of GDE2 was found in LAMP1-positive lysosomes **(Fig. S2)**. Quantification of the results from two independent neuronal cell lines confirmed that GDE2 predominantly localized to $Rab11^+$ endosomes (mean ~60%), somewhat less to $Rab5^+$ and $Rab4^+$ endosomes (mean 30-45%, depending on the cell line), and much less to $Rab7^+$ late endosomes and lysosomes (**Fig. 1D** and **Fig. S2**).

GDE2 interacts with Rab GTPases and undergoes constitutive endocytosis and recycling.
To validate the GDE2 localization data biochemically, we examined the interaction of GDE2 with relevant Rab GTPases in HEK293 cells. When GDE2 immuno-precipitates were blotted for Rab proteins, GDE2 was detected in complex with Rab4, Rab5, Rab7 and Rab11 (**Fig. 1E)**, in support of the co-localization results. We then measured the internalization and recycling of GDE2 using a biotin labeling procedure (**Fig. 1F**). GDE2-mCh-expressing N1E-115 cells were surface-labeled with NHS-SS-Biotin at 4° C and endocytosis was initiated by a temperature shift to 37° C. Cell-surface biotin was stripped and recycling of the internal GDE2 pool was allowed to proceed for 15 or 30 min. Lysates were precipitated using Streptavidin beads and GDE2 was eluted from the beads using anti-mCh antibody. As shown in **Fig. 1F**, internalized GDE2 was found to recycle back to the plasma membrane within 15-30 min. Of note, the GDE2 intracellular pool was not affected by serum stimulation (**Fig. 1F**). Similarly, GDE2 co-localization with Rab4, Rab5 and Rab11 was not altered in the presence of serum (Results not shown). We conclude that GDE2 endocytosis and recycling is a constitutive process, insensitive to serum factors.

C-terminal tail truncations of GDE2 disclose unique regulatory sequences.

Many integral membrane proteins contain linear sequence motifs that determine endocytosis, recycling or degradation (Bonifacino and Traub, 2003; Cullen and Steinberg, 2018). However, sequence inspection did not reveal canonical sorting motifs in the cytoplasmic regions of GDE2, such as tyrosine- or leucine-based motifs. To explore the sequence determinants of GDE2 trafficking we focused on the C-terminal tail (CT; aa 518-605) (**Fig. 2A**). Of note, the distal CT region of GDE2 shows marked sequence divergence among vertebrates. As shown in **Fig. 2A**, the aa 570-605 region is poorly conserved between mammalian, chicken and zebrafish GDE2, suggesting that the last 35 CT residues do not play a key regulatory role.

We made GDE2 CT truncations at aa 570, 560, 550, 540 and 530 (HA-tagged)**,** respectively (**Fig. 2A),** expressed them in N1E-115 cells and analyzed their co-localization with Rab5, Rab4 and Rab11. GDE2(ΔC570) showed the same subcellular localization as full-length GDE2, indicating that the last 35 CT residues (aa 571-605) are indeed dispensable for proper GDE2 localization and trafficking (**Fig. 2B**). GDE2(ΔC560) showed reduced surface expression (see also **Fig. 3C,D** below) and less Rab5 co-localization, while it preferentially accumulated in Rab4^{+} fast recycling endosomes at the expense of Rab11 co-localization (**Fig. 2B-F**). This suggests that the aa (561-570) region of GDE2 is required for endocytosis and, in particular, determines recycling pathway preference, shifting endocytosed GDE2 from slow to fast recycling. Strikingly, when truncated at aa 550, GDE2(ΔC550) accumulated at the plasma membrane, with little or no expression detected in early and recycling endosomes (**Fig. 2C-G**). It thus appears that the GDE2 aa (551-560) region is required for GDE2 endocytosis and consequent recycling.

Finally, when truncated at residue 530 or 540, GDE2(ΔC530) and GDE3(CΔ540) were no longer detected at the plasma membrane or endosomes, but remained trapped intracellularly as aggregates (**Fig. 2B-F** and **Fig. S3A,B**), suggestive of faulty expression and misfolding. Misfolded protein aggregates are usually routed to the autophagosome-lysosome degradation pathway. Indeed, GDE2(ΔC530) was found to accumulate in lysosomes (**Fig. S2**). We therefore conclude that the CT (aa 541-550) region is required for proper GDE2 expression, folding and transport through the early secretory pathway. The respective GDE2-Rab co-localizations are quantified in **Fig. 2F**. Together, these results disclose unique regulatory sequences in the GDE2 CT.

Localization of truncated GDE2 upon inducible expression

Quantification of GDE2 localization and activity in transiently transfected neuronal cells is a major challenge. We therefore turned to SH-SY5Y cells stably expressing doxycycline (Dox)-

inducible GDE2 (Matas-Rico et al., 2016). GDE2-HA constructs were analyzed for their expression upon Dox treatment during 12-48 hrs and for their subcellular localization. As shown in **Fig. 3A,** full-length (FL) GDE2, GDE2(ΔC570), GDE2(ΔC560) and catalytically dead GDE2(H233A) showed the same expression upon Dox treatment. The expression of GDE2(ΔC550) was somewhat reduced, whereas GDE2(ΔC540) and GDE2(ΔC530) were very poorly expressed (**Fig. 3A** and **Fig. S3**). Hence, the aa 540-550 region of GDE2 is essential for proper expression.

After Dox treatment (24 hrs) of SH-SY5Y cells, the GDE2 truncation mutants showed subcellular localizations similar to those in N1E-115 cells (**Fig. 3B**). We next measured surface levels of GDE2 and its mutants relative to their intracellular accumulation by quantitative analysis of confocal images (**Fig. 3C**); moreover, we quantified GDE2 surface levels by FACS analysis (**Fig. 3D**). From both figures, it is seen that GDE2-FL, GDE2(ΔC570) and GDE2(ΔC550) show similar surface levels, while GDE2(ΔC550) shows a much higher surface to cytoplasm ratio, consistent with its failure to undergo endocytosis. Finally, GDE2(ΔC560) showed reduced surface expression, consistent with its preferred accumulation recycling endosomes, particularly the Rab4$^+$ fast recycling ones (**Fig. 2F**)

GDE2 signaling activity: GPC6 shedding and induction of *NEUROD1* and *SNAP25*

Catalytic activity of GDE2 and its truncation mutants was measured by loss of GPC6 from the plasma membrane, using GDE2(H233A) as a negative control ((**Fig. 3D** and **Fig. S3C**). GPC6 is the only endogenously expressed glypican in SH-SY5Y cells (Matas-Rico et al., 2016). Activity of GDE2 and its truncation mutants towards GPC6 correlated with their respective surface levels, except for GDE2(ΔC560) (**Fig. 3D).** Strikingly, GDE2(ΔC560) was virtually inactive despite significant surface expression, but correlating with its preference for the Rab4$^+$ fast recycling pathway (**Fig. 2F**). This suggests that the aa 551-560 region negatively regulates GDE2 function. We next investigated GDE2-induced transcriptional responses in SH-SY5Y cells. GDE2 upregulates the expression of various neuronal differentiation markers, including *NEUROD1* and *SNAP25* (Matas-Rico et al., 2016). NEUROD1 is a transcription factor that drives both neurogenesis and pancreas development (Cho and Tsai, 2004), while *SNAP25* encodes a t-SNARE synaptic vesicle fusion protein (Kasai et al., 2012). How GPI-anchor surface cleavage leads to induction of neural differentiation genes is a key open question. We examined the expression of *NEUROD1* and *SNAP25* and found that their induction closely mirrored the degree of GPC6 shedding (**Fig. 3E**). GDE2(Δ570) was fully active, similar to GDE2-FL, as was the GDE2(Δ550) mutant that accumulates on the surface but lacks endocytosis and recycling competence. Strikingly again, GDE2(Δ560) showed hardly any transcriptional responses,

correlating with its lost ability to cleave GPC6, but at odds with its surface expression (**Fig. 3E**). **Fig. 4** summarizes our assignment of consecutive CT sequences to GDE2 secretion, endocytosis and recycling preference, as well as to negative regulation of GDE2 activity.

Discussion

Proper trafficking and surface localization of GDE2 is vital for its GPI-hydrolyzing activity and biological outcome. Our results disclose unique C-terminal sequences that determine GDE2 trafficking, surface expression and function, both positively and negatively. In summary (**Fig. 4**): (i) CT region (aa 541-550) is essential for proper expression, exocytosis and membrane insertion but lacks endocytosis information; (ii) region (aa 551-560) confers endocytosis and ensuing recycling competence with a clear preference for the Rab4$^+$ fast recycling route but, (iii), it renders GDE2 dysfunctional and thus qualifies as a negative regulatory sequence. Finally, the region (aa 561-570) is required for proper surface expression, endocytic recycling and biological activity, thus overriding negative regulation by upstream CT sequences. The finding that 10-aa sequence 551-EKLIFSEISD-560 confers loss of function to GDE2 is striking and warrants further investigation (**Fig. 4B**). One explanation could be that GDE2(Δ560), in contrast to GDE2(Δ570), prefers the Rab4$^+$ fast recycling pathway and is mislocalized to membrane nanodomains that are short of GPC6, resulting in loss of GDE2 function. In this light, it will be crucial to elucidate how, and precisely where, GDE2 recognizes and attacks its substrate(s), to which we have currently no clue.

The present findings should pave the way to a mechanistic understanding of GDE2 endocytic trafficking. In particular, it will be essential to identify adaptor proteins and effectors that interact with the GDE2 CT and drive the endocytic recycling machinery, such as the retromer and related multi-protein complexes (Burd and Cullen, 2014; Gautreau et al., 2014; McNally and Cullen, 2018), and map the critical CT residues involved.

In a broader context, the question arises how GDE2 function is regulated in addition its dynamic trafficking behavior. Under oxidative conditions, newly synthesized GDE2 is post-translationally modified and fails to enter the secretory pathway resulting in loss of function (Yan et al., 2015). Under physiological conditions, GDE2 catalytic activity could be controlled by as-yet-unknown binding partners and/or post-translational modifications, while its functional outcome will critically depend on the availability of specific substrates. Candidate GPI-anchored substrates that are known to determine neuronal fate include the neurodegenerative prion protein (PrPc), contactin

family proteins and neurotrophic receptors, all of which exist as soluble forms (Matas-Rico et al., 2017). Determining GDE2's substrate specificity has therefore high priority.

Regarding pathophysiological implications, GDE2 deficiency predicts poor prognosis in neuroblastoma (Matas-Rico et al., 2016), while loss of GDE2 causes progressive neurodegeneration in mice with pathologies analogous to human disease (Cave et al., 2017). This suggests that loss of GDE2 function might underlie aspects of human neurodegenerative disease and contribute to the pathogenesis of neuroblastoma. Yet, to our knowledge, disease-associated GDE2 dysfunction has not been documented to date, neither in neurodegenerative disease nor in nervous system malignancies. Given the present findings, however, GDE2 dysfunction could result from impaired endocytic trafficking rather than from loss-of-function mutations. Importantly, impaired trafficking is a hallmark of human neurodegenerative disease, including amyotrophic lateral sclerosis (ALS), Parkinson's and Alzheimer's disease (De Vos and Hafezparast, 2017; Kiral et al., 2018; McMillan et al., 2017; Schreij et al., 2016; Xu et al., 2018). It is therefore tempting to speculate that disease-associated defects in the endocytic sorting machinery, even if subtle, may lead to GDE2 mis-localization and thereby contribute to neurodegeneration and other disorders.

In conclusion, while GPI-anchor cleavage by cell-intrinsic ecto-phospholipases has long been understudied, our study is the first to define sequence determinants of GDE2 trafficking, localization and activity. It thus opens new avenues to elucidate how GDE2 function is normally regulated and explore its potential dysregulation in disease.

Experimental Procedures

Cells

SH-SY5Y, N1E-115 and HEK293 cells were grown in Dulbecco's modified Eagle's medium (DMEM) supplemented with 10% fetal bovine serum (FBS) at 37°C under 5% CO2. Antibodies used: anti-HA, 3F10 from Roche Diagnostics; β-Actin (AC-15) from Sigma; anti-mCh (16D7) was from Thermo Fisher; anti-EEA1 and LAMP-1 from Abcam; anti-GPC6 antibody LS-C36518 (LifeSpan Bioscience); APC anti-HA Epitope Tag Antibody (Biolegend); EZ-Link™ Sulfo-NHS-Biotin and Streptavidin Agarose Resins were from Pierce; GFP- or mCherry Trap® beads from ChomoTek; Fugene 6 from Invitrogen.

Plasmids and transfections

Human GDE2 cDNA was subcloned in pcDNA3.1 as described (Matas-Rico et al., 2016). Truncated versions of GDE2 were generated by amplification of full-length GDE2-HA or GDE2-mCherry using reverse primers for the last residues of each truncation. This was followed by a digestion with *BamH*I and *EcoR*V, after which the amplified inserts were cloned into digested and gel-purified pcDNA3.1, and selected by Ampicilin. GDE2 point mutants were generated by site-directed mutagenesis using two complementary oligonucleotides with the desired mutated bases at the center of their sequences. A temperature gradient from 55 to 60 degrees was used during the PCR amplifications. The PCR products were digested with *Dpn*I and transformed into DH5-α competent bacteria and screened for the expected mutated bases.

Confocal and super-resolution microscopy

Cells cultured on 24 mm, #1,5 coverslips were washed and fixed with 4% PFA, permeabilized with 0.1% Triton X-100 and blocked with 5% BSA for 1 hr. Incubation with primary antibodies was done for 1 hr, followed by incubation with Alexa-conjugated antibodies for 45 min at room temperature. For confocal microscopy, cells were washed with PBS, mounted with Immnuno- MountTM (Thermo Scientific) and visualized on a LEICA TCS-SP5 confocal microscopy (63x objective). Super-resolution imaging was done using an SR-GSD Leica microscope equipped with an oxygen scavenging system, as previously described (Matas-Rico et al., 2016). In short, 15000 frames were taken in TIRF or EPI mode at 10 ms exposure time. Movies were analyzed and corrected using the ImageJ plugin Thunderstorm (http://imagej.nih.gov/ij/), followed by correction with an ImageJ macro using the plugin Image Stabilizer.

Live-imaging

Live-cell imaging was done on a Leica TCS SP5 confocal microscope equipped with 63x oil immersion lens (numerical aperture 1.4; Leica, Mannheim, Germany). Coverslips were mounted on a metal ring system and exposed to buffer solution (140 mM, NaCl, 5 mM KCl, 2 mM MgCl2, 1 mM CaCl2, 23mM NaHCO3, 10 mM HEPES, 10 mM glucose). N1E-115 cells were selected randomly and images were collected at appropriate time intervals (5-15 sec). GDE2-mCh was visualized by exciting cells at 561 nm, while emission was detected at 610 ± 10 nm

GDE2 plasma membrane localization

We performed image analysis for plasma membrane localization of HA-tagged GDE2 constructs by using public domain software IMAGEJ. Shortly, confocal images stained for GDE2-HA were

segmented and analysed using Fiji software and a macro that automated the process. First, images were thresholded by the MaxEntropy algorithm to delimit single cells and filtered by Gaussian Blur (radius = 2) and smoothed for segmentation with a median radius of two. Using the Region of Interest manager on Fiji, the background was delimited by using the Li algorithm for thresholding. The cytoplasmic regions were selected by subtracting the plasma membrane thickness (fixed to 0.5 µm, but adjustable from a 0.2-5.0 range) and eroded with a pixel width of one to avoid having empty membranes in segmented cells. Next, the plasma membrane region was obtained by subtracting the background to the cytoplasmic region. Finally, the ratio membrane/cytoplasm was calculated from the median of these regions.

Western blotting

For Western blotting, cells were washed with cold PBS, lysed in NP-40 buffer supplemented with protease inhibitors and spun down. Protein concentration was measured using a BCA protein assay kit (Pierce) and LDS sample buffer (NuPAGE, Invitrogen) was added to the lysate or directly to the medium. Equal amounts were loaded on SDS-PAGE pre-cast gradient gels (4–12% Nu-Page Bis-Tris, Invitrogen), followed by transfer to nitrocellulose membrane. Non-specific protein binding was blocked by 5% skimmed milk in TBST; primary antibodies were incubated overnight at 4°C in TBST with 2.5% skimmed milk. Secondary antibodies conjugated to horseradish peroxidase (DAKO, Glostrup, Denmark) were incubated for 1 hr at room temperature; proteins were detected using ECL Western blot reagent.

Biotin labeling

For quantitation of GDE2 internalization and recycling, we used a biotin labeling assay. GDE2-mCh-expressing N1E-115 cells were serum starved for 1hr., transferred to ice, washed in ice-cold PBS, and surface labeled at 4°C with 0.2 mg/ml NHS-SS-biotin (Pierce). For GDE2 internalization, cells were exposed to serum-free medium at 37°C for the indicated time periods. Cells were transferred to ice and washed with PBS, remaining surface biotin was reduced with sodium 2-mercaptoethane sulfonate (MesNa), and the reaction was quenched with iodoacetamide (IAA) prior to cell lysis. For recycling assays, cells were labeled with biotin as above, and incubated in serum-free medium at 37°C for 30 min to allow internalization of GDE2. Cells were returned to ice, washed with PBS, and biotin was reduced using MesNa. Recycling of the internal GDE2 pool was induced by a temperature shift to 37°C for 0–30 min. Cells were returned to ice, washed with PBS and surface biotin was reduced by MesNa. MesNa was quenched by IAA and the cells were lysed. Biotin-labeled GDE2 was detected using Streptavidin beads and anti-mCh antibody.

Immunoprecipitation

For co-immunoprecipitation of GDE2 and Rabs, HEK293Tcells were plated on plastic dishes of 10 cm diameter and transient co-transfected with GDE2-mCh or –GFP and Rab4-GFP, Rab5-mCh, Rab7-GFP or Rab11-mCh. After 24 hrs cells were lysed using RIPA buffer. Protein concentration was determined using Protein BCA protein assay kit (Pierce). Immunoprecipitation was carried out incubating 500 µg - 1 mg cytoplasmic extracts with GFP- or mCherry Trap® beads(ChomoTek) at 4°C for 1hr. Beads were washed three times and eluted by boiling in SDS sample buffer for 10 min. at 95°C. Supernatants were applied onto an SDS gel and subjected to immunoblot analysis

Inducible GDE2 expression

SH-SY5Y cells with inducible expression of GDE2 constructs were generated using the Retro-X™ Tet-On® Advanced Inducible Expression System (ClonTech), as described (Matas-Rico et al., 2016). After retroviral transduction, the cells were placed under selection with G418 (800 mg/ml) supplemented with puromycin (1 μg/ml) for 10 days. GDE2 induction (in the presence of 1 μg/ml doxycycline) was verified by Western blot and confocal microscopy. Transient transfection was performed with Fugene 6 reagent (Invitrogen) according to the manufacturer's instructions.

Flow Cytometry

For GPC6 and GDE2-HA surface expression analysis, cells were grown in complete medium with 10% FCS with or without doxycycline. Cells were trypsinized into single-cell suspensions and then $8x10^5$ cells were incubated with 5 µl of anti-GPC6 antibody LS-C36518 (LifeSpan Bioscience) and in 4 µl of APC anti-HA antibody (Biolegend). Bound GPC6 antibody were detected by incubating with a 1:200 dilution of goat anti-mouse Alexa-488 secondary antibody in 2% BSA for 45 min on ice. Fluorescence measurements were performed using BD LSRFORTESSA and using Flow Jo software.

Induction of *NEUROD1* and *SNAP25*

Total RNA was extracted using the GeneJET purification kit (Fermentas). cDNA was synthesized by reverse transcription from 5 µg RNA using First Strand cDNA Syntesis Kit (Thermo Scientific). RTqPCR was performed on a 7500 Fast System (Applied Biosystems) as follows: 95°C for 2 min, 95 ^{o}C for 0 min., 40 cycles at 95°C for 15 sec. followed by 60°C for 1 min. for annealing and extension. The final reaction mixtures (20 µl) consisted of diluted cDNA, 16SYBR Green Supermix (Applied Biosystems), 200 nM forward primer and 200 nM reverse primer. Reactions were performed in 96-well plates in triplo. The primers used are: NEUROD1, forward: CCGACAGAGCCCAGATGTAGTTCTT and reverse: GCCCCAGGGTTATGAGACTATCACT; SNAP25, forward: AGTTGGCTGATGAGTCGCTG and reverse: TGAAAAGGCCACAGCATTTC; cyclophilin, forward: CATCTGCACTGCCAAGACTGA and reverse: TTGCCAAACACCACATGCTT. As a negative control, the cDNA was replaced by milliQ. Cyclophilin was used as reference gene. Each sample was analyzed in triplo. The normalized expression (NE) data were calculated by the equation NE= 2(Ct target – Ct reference).

Supplemental Information

Supplemental Information includes one movie and three figures.

Author Contributions

F.S.-P., M.v.V., B.v.d.B., D.L.-P., R.B. and E.M.-R. conceived and performed experiments. A.P., W.H.M., and E.M.-R. supervised the work. W.H.M wrote the manuscript with feedback from F.S.-P., A.P., and E.M.-R.

Acknowledgments

This study was funded by the Dutch Cancer Society (KWF; project 2017-10215 "Membrane glycerophosphodiesterases: novel players in cell differentiation and cancer biology").

References

Bonifacino, J.S., and L.M. Traub. 2003. Signals for sorting of transmembrane proteins to endosomes and lysosomes. *Annual review of biochemistry*. 72:395-447.

Burd, C., and P.J. Cullen. 2014. Retromer: a master conductor of endosome sorting. *Cold Spring Harb Perspect Biol*. 6.

Cave, C., S. Park, M. Rodriguez, M. Nakamura, A. Hoke, M. Pletnikov, and S. Sockanathan. 2017. GDE2 is essential for neuronal survival in the postnatal mammalian spinal cord. *Mol Neurodegener*. 12:8.

Cho, J.H., and M.J. Tsai. 2004. The role of BETA2/NeuroD1 in the development of the nervous system. *Molecular neurobiology*. 30:35-47.

Corda, D., T. Kudo, P. Zizza, C. Iurisci, E. Kawai, N. Kato, N. Yanaka, and S. Mariggio. 2009. The developmentally regulated osteoblast phosphodiesterase GDE3 is glycerophosphoinositol-specific and modulates cell growth. *J Biol Chem*. 284:24848-24856.

Corda, D., M.G. Mosca, N. Ohshima, L. Grauso, N. Yanaka, and S. Mariggio. 2014. The emerging physiological roles of the glycerophosphodiesterase family. *The FEBS journal*. 281:998-1016.

Cullen, P.J., and F. Steinberg. 2018. To degrade or not to degrade: mechanisms and significance of endocytic recycling. *Nat Rev Mol Cell Biol*. 19:679-696.

De Vos, K.J., and M. Hafezparast. 2017. Neurobiology of axonal transport defects in motor neuron diseases: Opportunities for translational research? *Neurobiology of disease*. 105:283-299.

Ferguson, M.A.J., G.W. Hart, and T. Kinoshita. 2015. Glycosylphosphatidylinositol Anchors. *In* Essentials of Glycobiology. rd, A. Varki, R.D. Cummings, J.D. Esko, P. Stanley, G.W. Hart, M. Aebi, A.G. Darvill, T. Kinoshita, N.H. Packer, J.H. Prestegard, R.L. Schnaar, and P.H. Seeberger, editors, Cold Spring Harbor (NY). 137-150.

Fujita, M., and T. Kinoshita. 2010. Structural remodeling of GPI anchors during biosynthesis and after attachment to proteins. *FEBS letters*. 584:1670-1677.

Gallazzini, M., J.D. Ferraris, and M.B. Burg. 2008. GDPD5 is a glycerophosphocholine phosphodiesterase that osmotically regulates the osmoprotective organic osmolyte GPC. *Proc Natl Acad Sci U S A*. 105:11026-11031.

Gautreau, A., K. Oguievetskaia, and C. Ungermann. 2014. Function and regulation of the endosomal fusion and fission machineries. *Cold Spring Harb Perspect Biol*. 6.

Hutagalung, A.H., and P.J. Novick. 2011. Role of Rab GTPases in membrane traffic and cell physiology. *Physiological reviews*. 91:119-149.

Kasai, H., N. Takahashi, and H. Tokumaru. 2012. Distinct initial SNARE configurations underlying the diversity of exocytosis. *Physiological reviews*. 92:1915-1964.

Kiral, F.R., F.E. Kohrs, E.J. Jin, and P.R. Hiesinger. 2018. Rab GTPases and Membrane Trafficking in Neurodegeneration. *Curr Biol*. 28:R471-R486.

Langemeyer, L., F. Frohlich, and C. Ungermann. 2018. Rab GTPase Function in Endosome and Lysosome Biogenesis. *Trends in cell biology*. 28:957-970.

Low, M.G., and K.S. Huang. 1991. Factors affecting the ability of glycosylphosphatidylinositol-specific phospholipase D to degrade the membrane anchors of cell surface proteins. *The Biochemical journal*. 279 (Pt 2):483-493.

Matas-Rico, E., M. van Veen, D. Leyton-Puig, J. van den Berg, J. Koster, K.M. Kedziora, B. Molenaar, M.J. Weerts, I. de Rink, R.H. Medema, B.N. Giepmans, A. Perrakis, K. Jalink, R. Versteeg, and W.H. Moolenaar. 2016. Glycerophosphodiesterase GDE2 Promotes Neuroblastoma Differentiation through Glypican Release and Is a Marker of Clinical Outcome. *Cancer Cell*. 30:548-562.

Matas-Rico, E., M. van Veen, and W.H. Moolenaar. 2017. Neuronal differentiation through GPI-anchor cleavage. *Cell cycle*. 16:388-389.

Maxfield, F.R., and T.E. McGraw. 2004. Endocytic recycling. *Nature Reviews Molecular Cell Biology*. 5:121.

Mayle, K.M., A.M. Le, and D.T. Kamei. 2012. The intracellular trafficking pathway of transferrin. *Biochim Biophys Acta*. 1820:264-281.

McMillan, K.J., H.C. Korswagen, and P.J. Cullen. 2017. The emerging role of retromer in neuroprotection. *Current opinion in cell biology*. 47:72-82.

McNally, K.E., and P.J. Cullen. 2018. Endosomal Retrieval of Cargo: Retromer Is Not Alone. *Trends in cell biology*. 28:807-822.

Metz, C.N., G. Brunner, N.H. Choi-Muira, H. Nguyen, J. Gabrilove, I.W. Caras, N. Altszuler, D.B. Rifkin, E.L. Wilson, and M.A. Davitz. 1994. Release of GPI-anchored membrane proteins by a cell-associated GPI-specific phospholipase D. *The EMBO journal*. 13:1741-1751.
Ohshima, N., T. Kudo, Y. Yamashita, S. Mariggio, M. Araki, A. Honda, T. Nagano, C. Isaji, N. Kato, D. Corda, T. Izumi, and N. Yanaka. 2015. New members of the mammalian glycerophosphodiester phosphodiesterase family: GDE4 and GDE7 produce lysophosphatidic acid by lysophospholipase D activity. *J Biol Chem*. 290:4260-4271.
Park, S., C. Lee, P. Sabharwal, M. Zhang, C.L. Meyers, and S. Sockanathan. 2013. GDE2 promotes neurogenesis by glycosylphosphatidylinositol-anchor cleavage of RECK. *Science*. 339:324-328.
Paulick, M.G., and C.R. Bertozzi. 2008. The glycosylphosphatidylinositol anchor: a complex membrane-anchoring structure for proteins. *Biochemistry*. 47:6991-7000.
Schreij, A.M., E.A. Fon, and P.S. McPherson. 2016. Endocytic membrane trafficking and neurodegenerative disease. *Cellular and molecular life sciences : CMLS*. 73:1529-1545.
Scott, C.C., F. Vacca, and J. Gruenberg. 2014. Endosome maturation, transport and functions. *Seminars in cell & developmental biology*. 31:2-10.
van Veen, M., L.A. Mans, E. Matas-Rico, J. van Pelt, A. Perrakis, W.H. Moolenaar, and A.G. Haramis. 2018. Glycerophosphodiesterase GDE2/GDPD5 affects pancreas differentiation in zebrafish. *The international journal of biochemistry & cell biology*. 94:71-78.
van Veen, M., E. Matas-Rico, K. van de Wetering, D. Leyton-Puig, K.M. Kedziora, V. De Lorenzi, Y. Stijf-Bultsma, B. van den Broek, K. Jalink, N. Sidenius, A. Perrakis, and W.H. Moolenaar. 2017. Negative regulation of urokinase receptor activity by a GPI-specific phospholipase C in breast cancer cells. *eLife*. 6.
Wandinger-Ness, A., and M. Zerial. 2014. Rab proteins and the compartmentalization of the endosomal system. *Cold Spring Harb Perspect Biol*. 6:a022616.
Xu, W., F. Fang, J. Ding, and C. Wu. 2018. Dysregulation of Rab5-mediated endocytic pathways in Alzheimer's disease. *Traffic*. 19:253-262.
Yan, Y., C. Wladyka, J. Fujii, and S. Sockanathan. 2015. Prdx4 is a compartment-specific H2O2 sensor that regulates neurogenesis by controlling surface expression of GDE2. *Nature communications*. 6:7006.

Figure Legends

Figure 1. GDE2 localization and endocytic trafficking routes

A. Domain structure of GDE2 showing six transmembrane (TM) domains, a GDPD ectodomain and intracellular N- and C-terminal tails.

B. GDE2 cleaves and sheds GPI-anchored proteins resulting activation of signaling cascades.

C. GDE2 subcellular localization. Top: Confocal images showing GDE2-GFP in membrane microdomains and intracellular vesicles in N1E-115 and SH-SY5Y cells; bar, 10 μm. Bottom: Super-resolution images of N1E-115 cells expressing GDE2-GFP. White arrows point to membrane microdomains. Bar, 1 μm.

D. Confocal images of GDE2 in early, recycling and late endosomes, Rab5-, Rab11-, Rab4-, and Rab7-positive, respectively, in SH-SY5Y cells maintained in serum-free medium. Bar, 10 μm. Bottom panels show quantification of GDE2 co-localization with the indicated Rab GTPases, expressed as the percentage of yellow versus red pixels (≥25 cells from three independent experiments).

E. GDE2 (fused to GFP or mCh) associates with the indicated Rab GTPases in HEK293T cells. GDE2 was immunoprecipitated (IP) and subjected to immunoblotting (IB) using either anti-GFP or anti-mCh antibody.

F. Top panel: Schematic illustration of the internalization and recycling assay using biotin labelling. N1E-115 cells expressing GDE2-mCh were surface-labelled with NHS-S-S-Biotin. Internalization proceeded for 15 and 30 min at 37˚C in presence or absence of 10% FBS. Surface biotin was reduced with MesNa at 4˚C, and the cells were shifted to 37˚C for the indicated time periods (with 10% FBS) to trigger recycling of the internal pool. Bottom panel: The amount of internalized and total biotin-labelled GDE2 determined by immuno-blotting using anti-mCh antibody. Actin was used as loading control.

Figure 2. Progressive GDE2 CT truncations reveal trafficking determinants.

A. GDE2 CT sequence alignments of human, mouse, chicken and zebrafish GDE2, and the truncations made in hGDE2.

B. Subcellular localization of GDE2-HA and its truncation mutants in N1E-115 cells. Bar, 10 μm.

C,D,E. Confocal images of N1E-115 cells co-expressing the indicated GDE2 CT truncations and Rab5-mCh (**C**), Rab4-GFP (**D**) and Rab11-mCh (**E**). Bar, 10 μm.

F. Quantification of GDE2-Rab co-localization (percentage of yellow versus red pixels for ≥25 cells from three independent experiments).

Figure 3. Induced expression of GDE2 truncation mutants in SH-SY5Y cells: localization, GPC6 shedding and induction of differentiation markers.

A. Immunoblots showing expression of HA-tagged full-length (FL) GDE2 and the indicated truncated versions in doxycyclin (Dox)-inducible SH-SY5Y cells during 12-48 hrs. Actin was used as loading control.

B. Localization of GDE2 and the indicated CT truncation construct in Dox-treated SH-SY5Y cells (24 hrs).

C. Quantification of GDE2 surface versus cytosol localization in inducible SH-SY5Y cells (24 hrs). At least 20 cells from three independent preparations were segmented and analysed by IMAGEJ to calculate the membrane/cytoplasmic ratio (median ± SEM); ***p<0.001, ****p<0.0001, unpaired t test.

D. Left panel, Endogenous GPC6 levels upon Dox-induced (24 hrs) expression of GDE2 and its truncated mutants, compared to GDE2-deficient cells (-Dox), detected by flow cytometry using GPC6 antibody. Right panel, Surface expression of GDE2-HA and GPC6 under the same conditions, detected by flow cytometry. Quantifications (mean ± SEM) of the above FACS data from three independent experiments; *p<0.05; **p<0.01, paired t test.

E. Induction of *NEUROD1* and *SNAP25* upon Dox-induced (24 hrs) expression of the indicated GDE2 constructs as determined by qPCR. Inactive GDE2(H233A) was used as negative control.

Figure 4. Sequence determinants of GDE2 trafficking and signalling efficacy.

A. The CT region (aa 530/541-550) is essential for proper expression, secretion and membrane insertion. Sequence (aa 551-560) determines endocytosis and Rab4 fast recycling preference, but also negatively regulates GDE2 function at the surface. Sequence (561-570) is required for proper GDE2 recycling and function. The last CT 35 residues (aa 571-605) are dispensable for GDE2 function. Residues in white are not conserved between mammalian, chicken and/or zebrafish GDE2 (see **Fig. 2A**).

B. Scheme of membrane trafficking, localization and signalling output of GDE2 and the indicated truncation mutants. GDE2 is constitutively internalized while the majority of endocytosed GDE2 traffics along Rab4$^+$ and Rab11$^+$ recycling routes in a sequence-dependent manner, with Rab4+ recycling being the preferred route of GDE2(ΔC560). A smaller part of GDE2 is routed to Rab7$^+$ late endosomes for lysosomal degradation. Signalling efficacy is inferred from GPC6 shedding cleavage and induction of *NEUROD1* and *SNAP25*. Note dysfunction of GDE2(ΔC560). Disease-associated trafficking defects may similarly lead to GDE2 dysfunction. See Discussion.

Supplemental Information

Movie S1. Live imaging of GDE2-containing vesicle movements in SH-SY5Y cells.

Figure 1

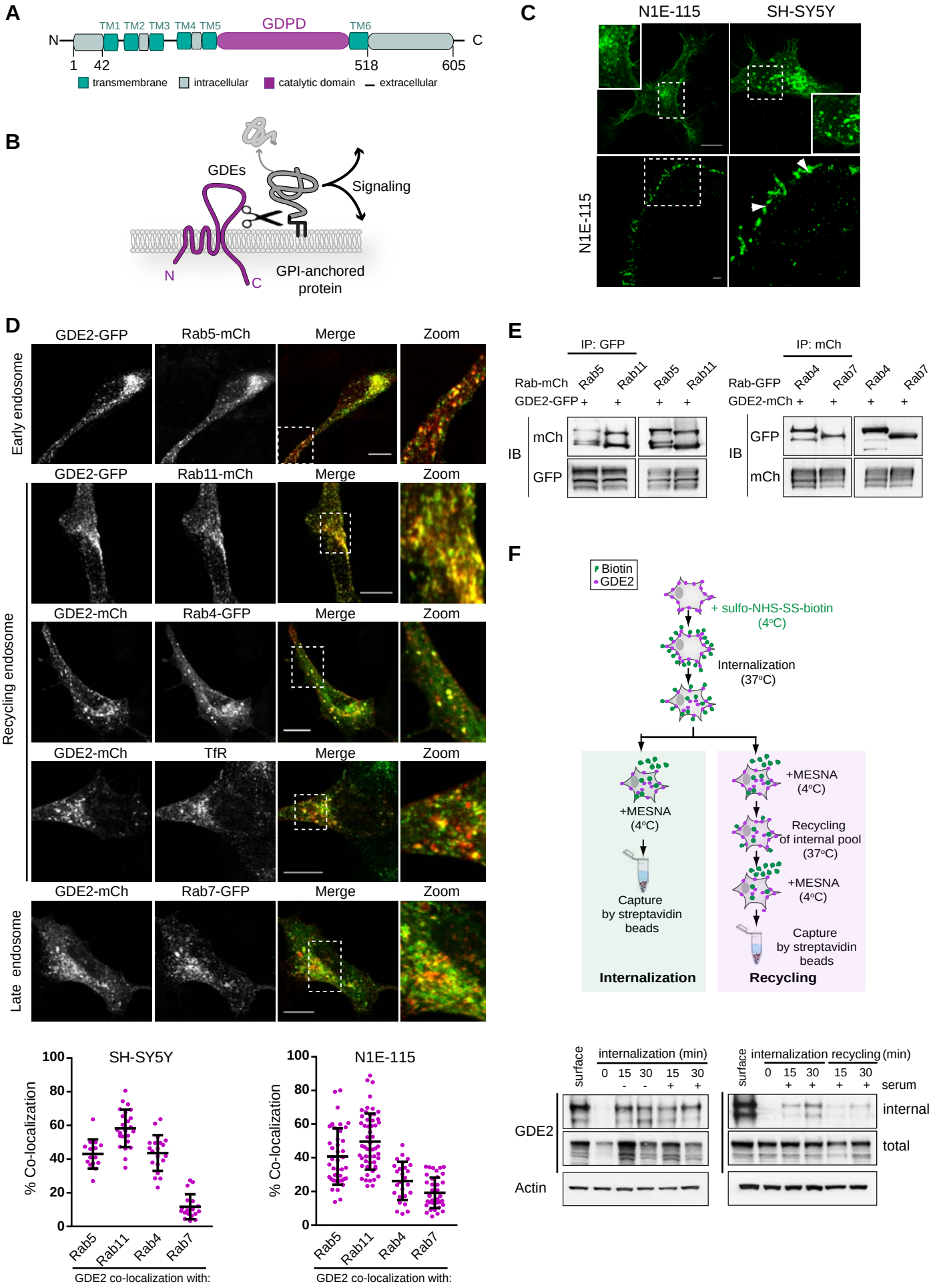
A
N
TM1 TM2 TM3 TM4 TM5
GDPD
TM6
C
1 42 518 605
transmembrane
intracellular
catalytic domain
extracellular
B
GDEs
Signaling
N
C
GPI-anchored protein
C
N1E-115
SH-SY5Y
N1E-115
D
GDE2-GFP
Rab5-mCh
Merge
Zoom
Early endosome
GDE2-GFP
Rab11-mCh
Merge
Zoom
GDE2-mCh
Rab4-GFP
Merge
Zoom
GDE2-mCh
TfR
Merge
Zoom
Recycling endosome
GDE2-mCh
Rab7-GFP
Merge
Zoom
Late endosome
SH-SY5Y
% Co-localization
Rab5
Rab11
Rab4
Rab7
GDE2 co-localization with:
N1E-115
% Co-localization
Rab5
Rab11
Rab4
Rab7
GDE2 co-localization with:
E
IP: GFP
Rab-mCh
Rab5
Rab11
Rab5
Rab11
GDE2-GFP
IB
mCh
GFP
IP: mCh
Rab-GFP
Rab4
Rab7
Rab4
Rab7
GDE2-mCh
IB
GFP
mCh
F
Biotin
GDE2
+ sulfo-NHS-SS-biotin (4°C)
Internalization (37°C)
+MESNA (4°C)
Capture by streptavidin beads
Internalization
+MESNA (4°C)
Recycling of internal pool (37°C)
+MESNA (4°C)
Capture by streptavidin beads
Recycling
surface
internalization (min)
0 15 30 15 30
- - + +
GDE2
Actin
surface
internalization recycling (min)
0 15 30 15 30
+ + + +
serum
internal
total

Figure 2

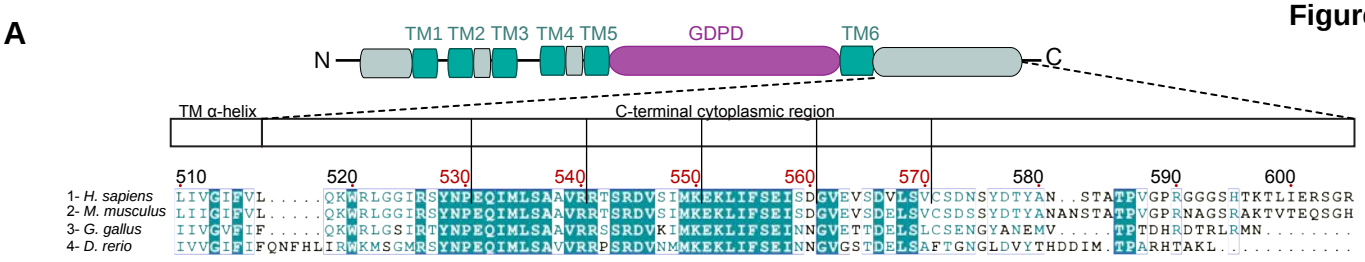
A
TM1 TM2 TM3 TM4 TM5
GDPD
TM6
N
C
TM α-helix
C-terminal cytoplasmic region
510 520 530 540 550 560 570 580 590 600
1- H. sapiens
2- M. musculus
3- G. gallus
4- D. rerio

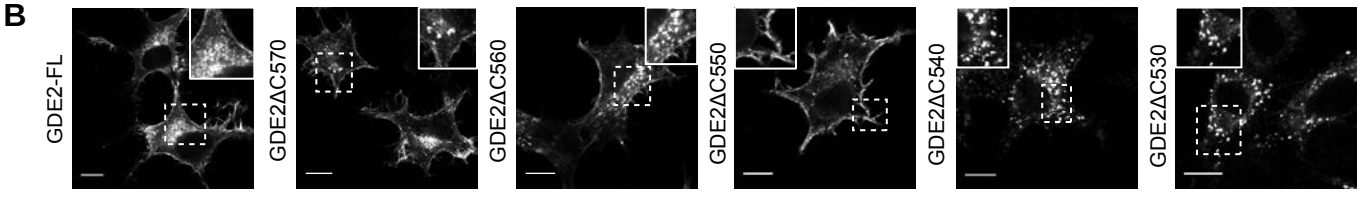
B
GDE2-FL
GDE2ΔC570
GDE2ΔC560
GDE2ΔC550
GDE2ΔC540
GDE2ΔC530

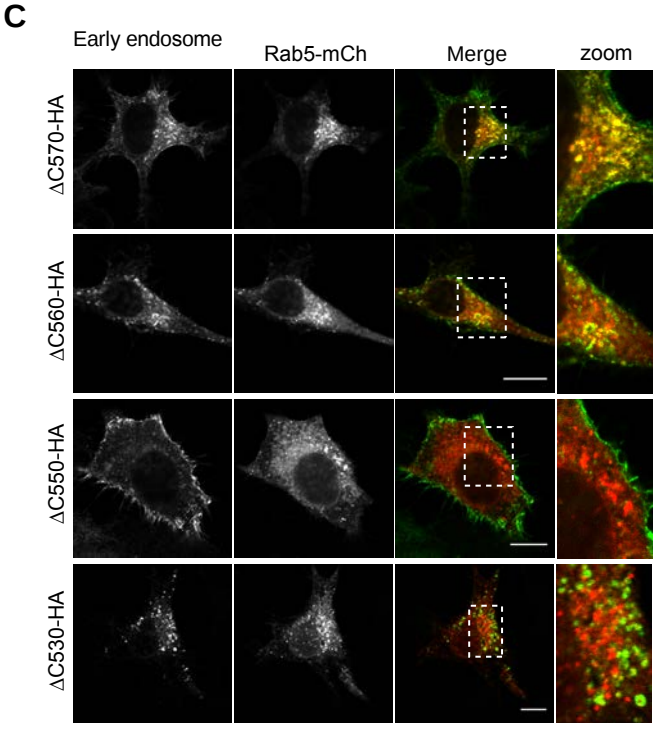
C
Early endosome
Rab5-mCh
Merge
zoom
ΔC570-HA
ΔC560-HA
ΔC550-HA
ΔC530-HA

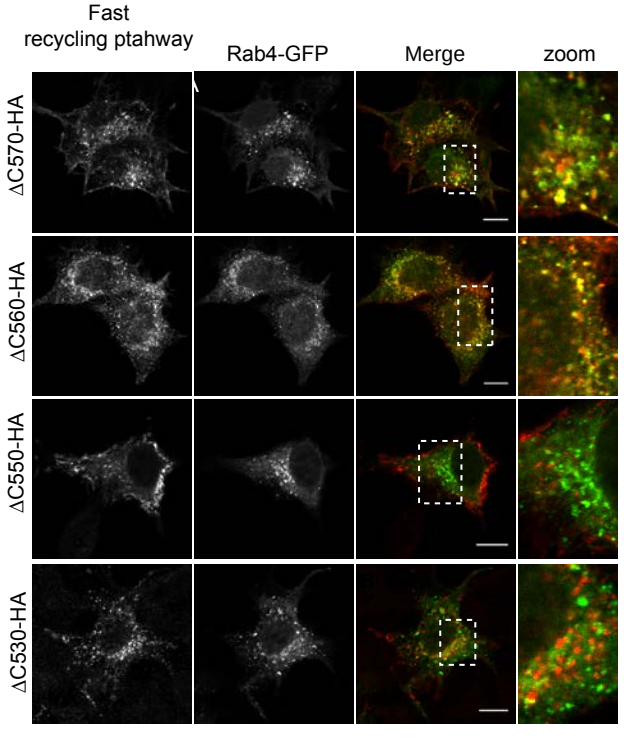
D
Fast recycling ptahway
Rab4-GFP
Merge
zoom
ΔC570-HA
ΔC560-HA
ΔC550-HA
ΔC530-HA

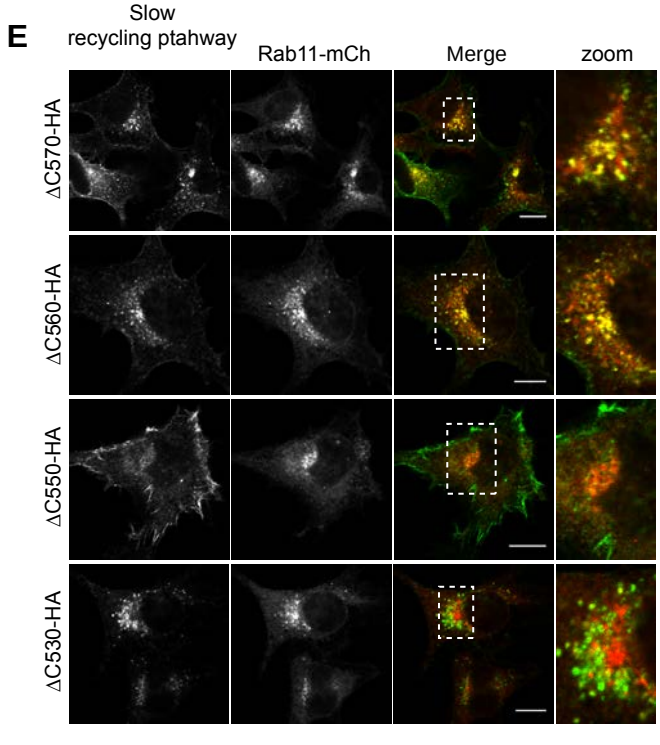
E
Slow recycling ptahway
Rab11-mCh
Merge
zoom
ΔC570-HA
ΔC560-HA
ΔC550-HA
ΔC530-HA

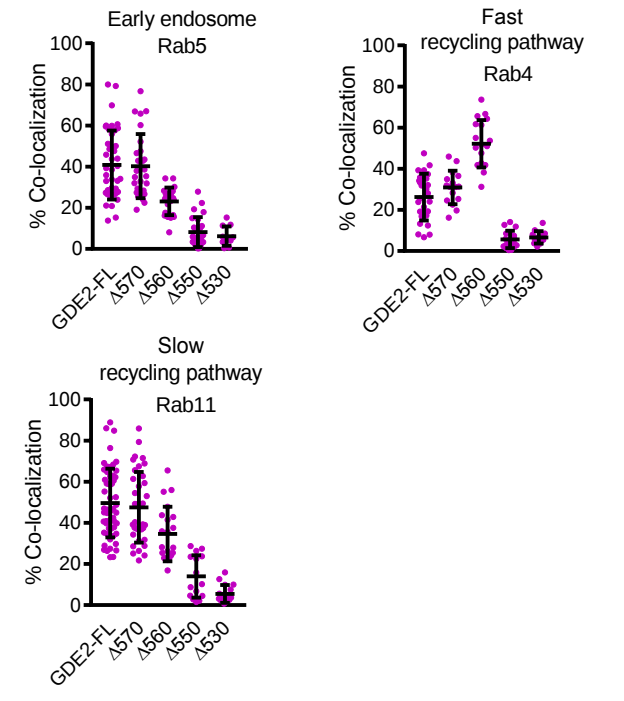
F
Early endosome
Rab5
Fast recycling pathway
Rab4
Slow recycling pathway
Rab11
% Co-localization
0
20
40
60
80
100
GDE2-FL
Δ570
Δ560
Δ550
Δ530

Figure 3

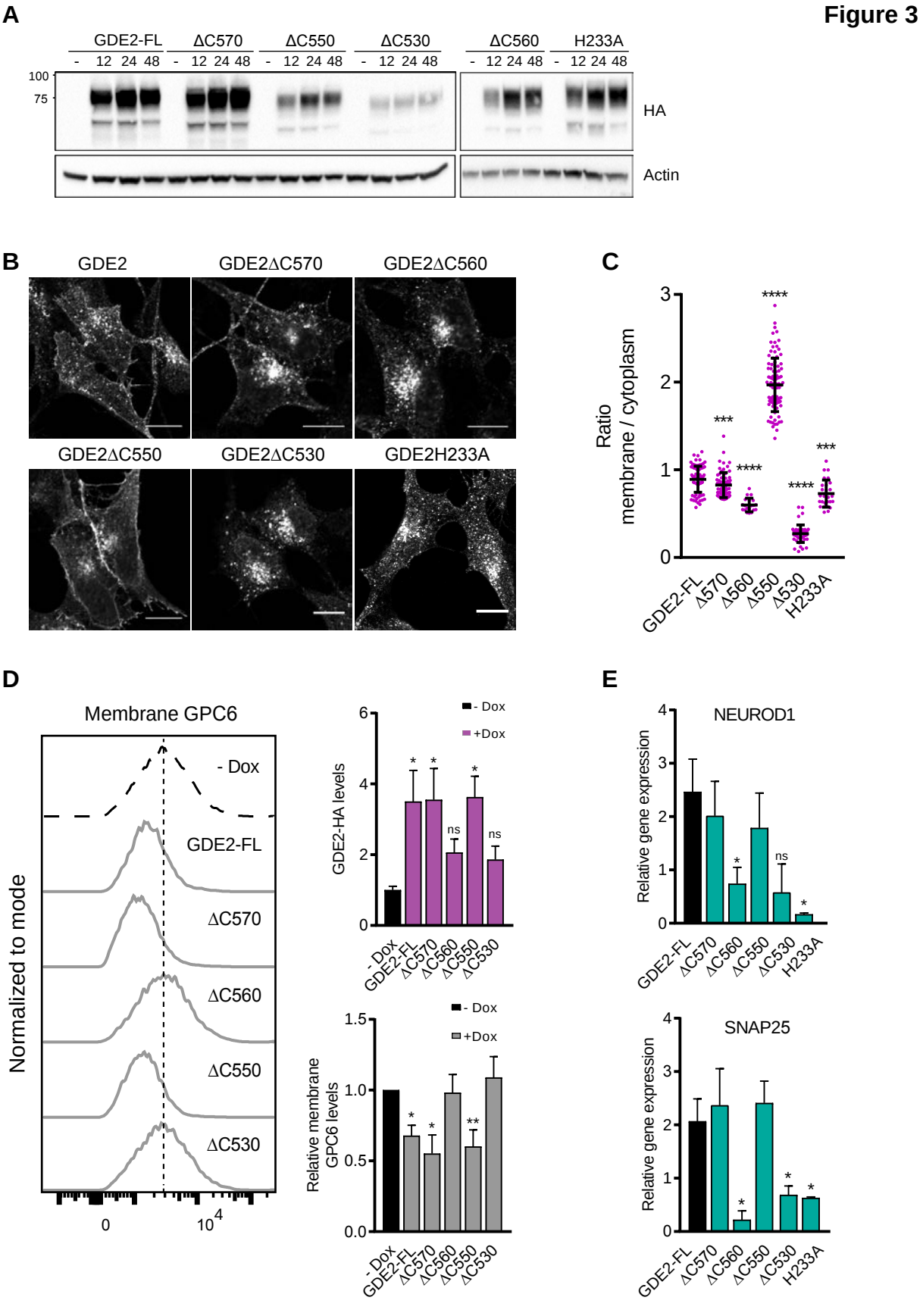
A
GDE2-FL
ΔC570
ΔC550
ΔC530
ΔC560
H233A
- 12 24 48
100
75
HA
Actin
B
GDE2
GDE2ΔC570
GDE2ΔC560
GDE2ΔC550
GDE2ΔC530
GDE2H233A
C
Ratio membrane / cytoplasm
GDE2-FL
Δ570
Δ560
Δ550
Δ530
H233A
D
Membrane GPC6
- Dox
GDE2-FL
ΔC570
ΔC560
ΔC550
ΔC530
Normalized to mode
GDE2-HA levels
Relative membrane GPC6 levels
+Dox
E
NEUROD1
SNAP25
Relative gene expression

Figure 4

A

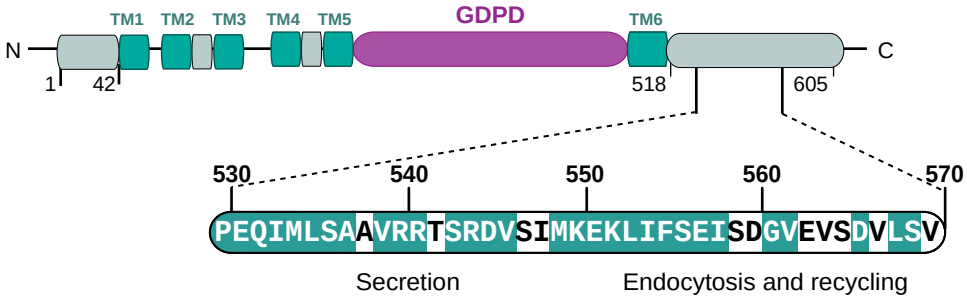
TM1
TM2
TM3
TM4
TM5
GDPD
TM6
N
C
1
42
518
605
530
540
550
560
570
PEQIMLSAAVRRTSRDVSIMKEKLIFSEISDGVEVSDVLSV
Secretion
Endocytosis and recycling

B

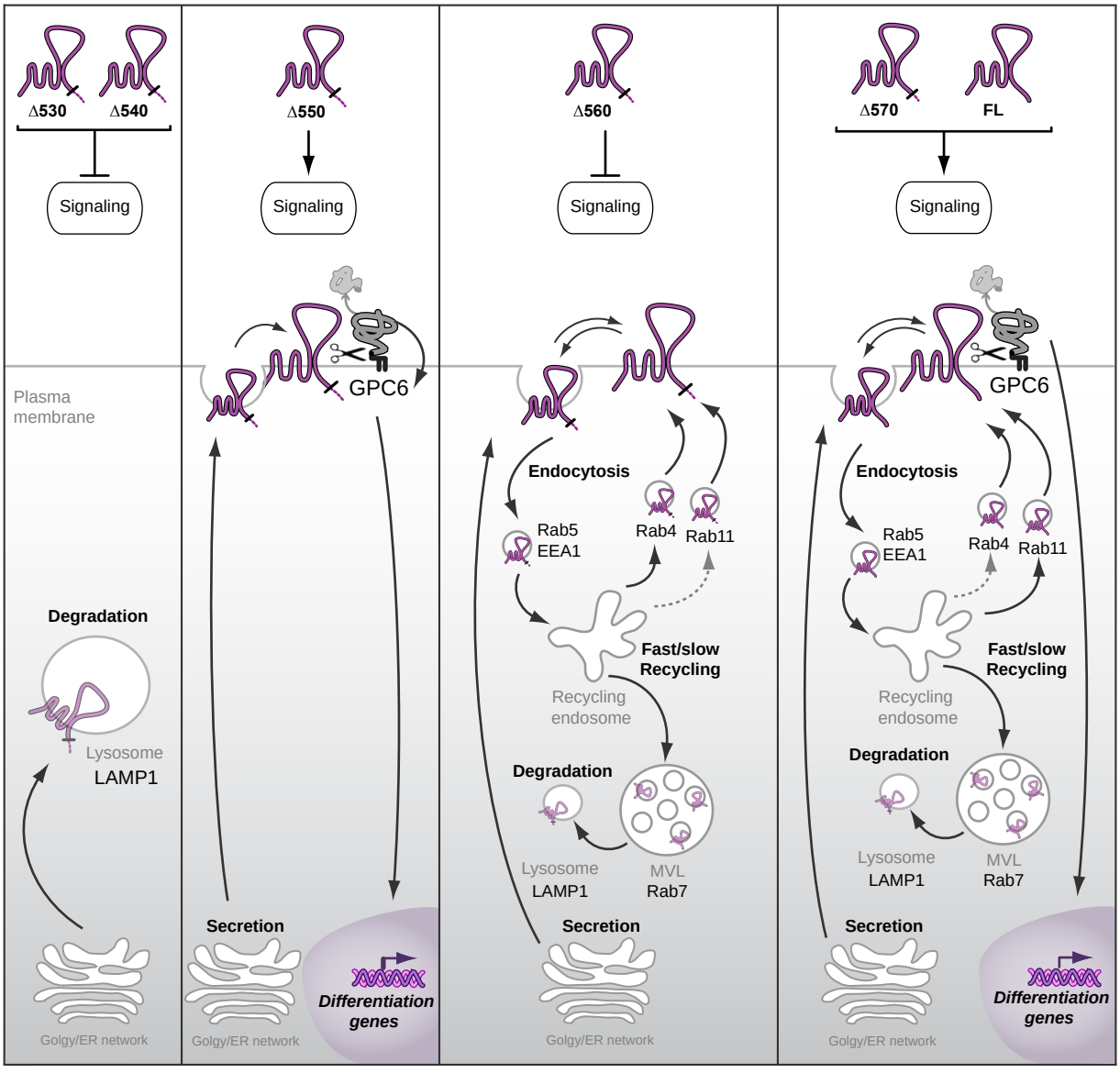
Δ530
Δ540
Δ550
Δ560
Δ570
FL
Signaling
Signaling
Signaling
Signaling
GPC6
GPC6
Plasma membrane
Endocytosis
Endocytosis
Rab5
EEA1
Rab4
Rab11
Rab5
EEA1
Rab4
Rab11
Degradation
Lysosome
LAMP1
Fast/slow Recycling
Recycling endosome
Fast/slow Recycling
Recycling endosome
Degradation
Degradation
Lysosome
LAMP1
MVL
Rab7
Lysosome
LAMP1
MVL
Rab7
Secretion
Secretion
Secretion
Golgy/ER network
Golgy/ER network
Golgy/ER network
Golgy/ER network
Differentiation genes
Differentiation genes

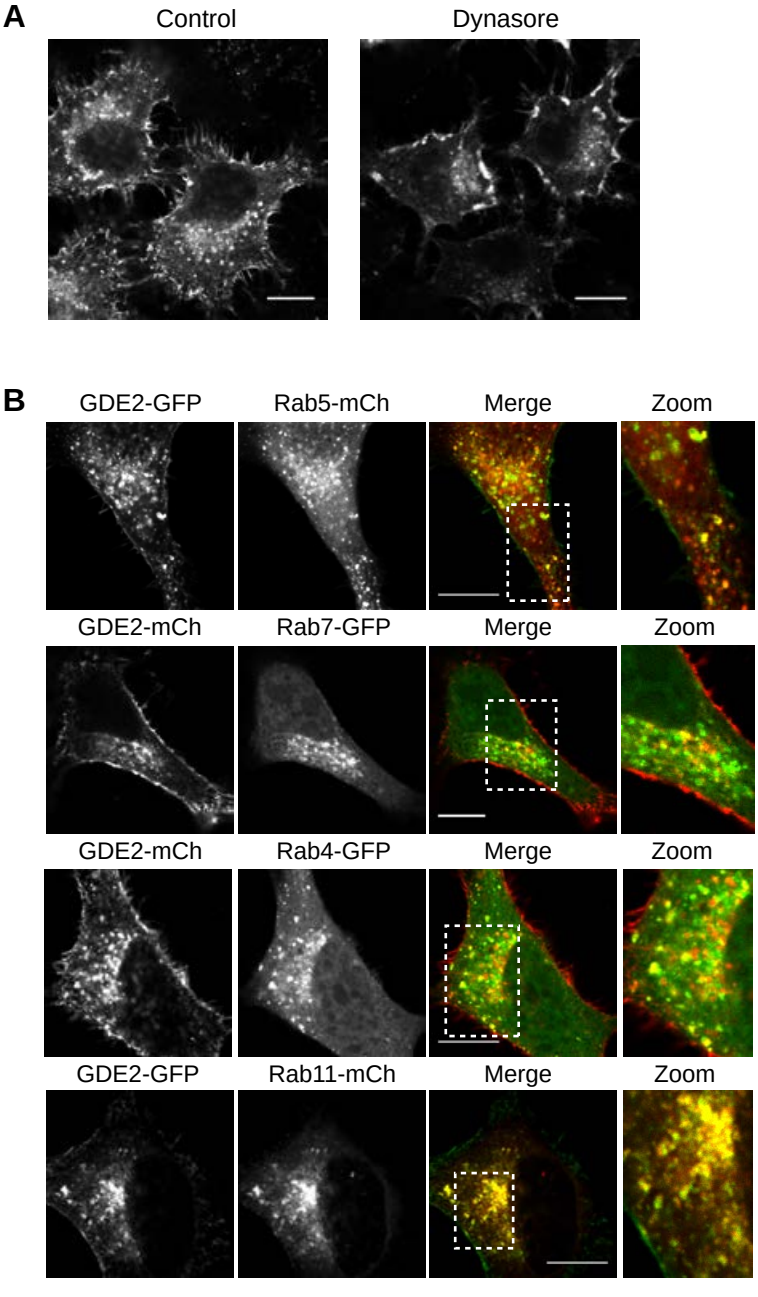

Figure S1. GDE2 subcellular localization in N11E-115 cells
A. GDE2 accumulates at the cell surface with loss of GDE2-positive vesicles in N1E-115 cells treated with the dynamin inhibitor Dynasore (80 µM). Bar, 10 µm.
B. GDE2 co-localization with the indicated Rab GTPases in N1E-115 cells. Bar, 10 µm. See Fig. 1D and text for details.

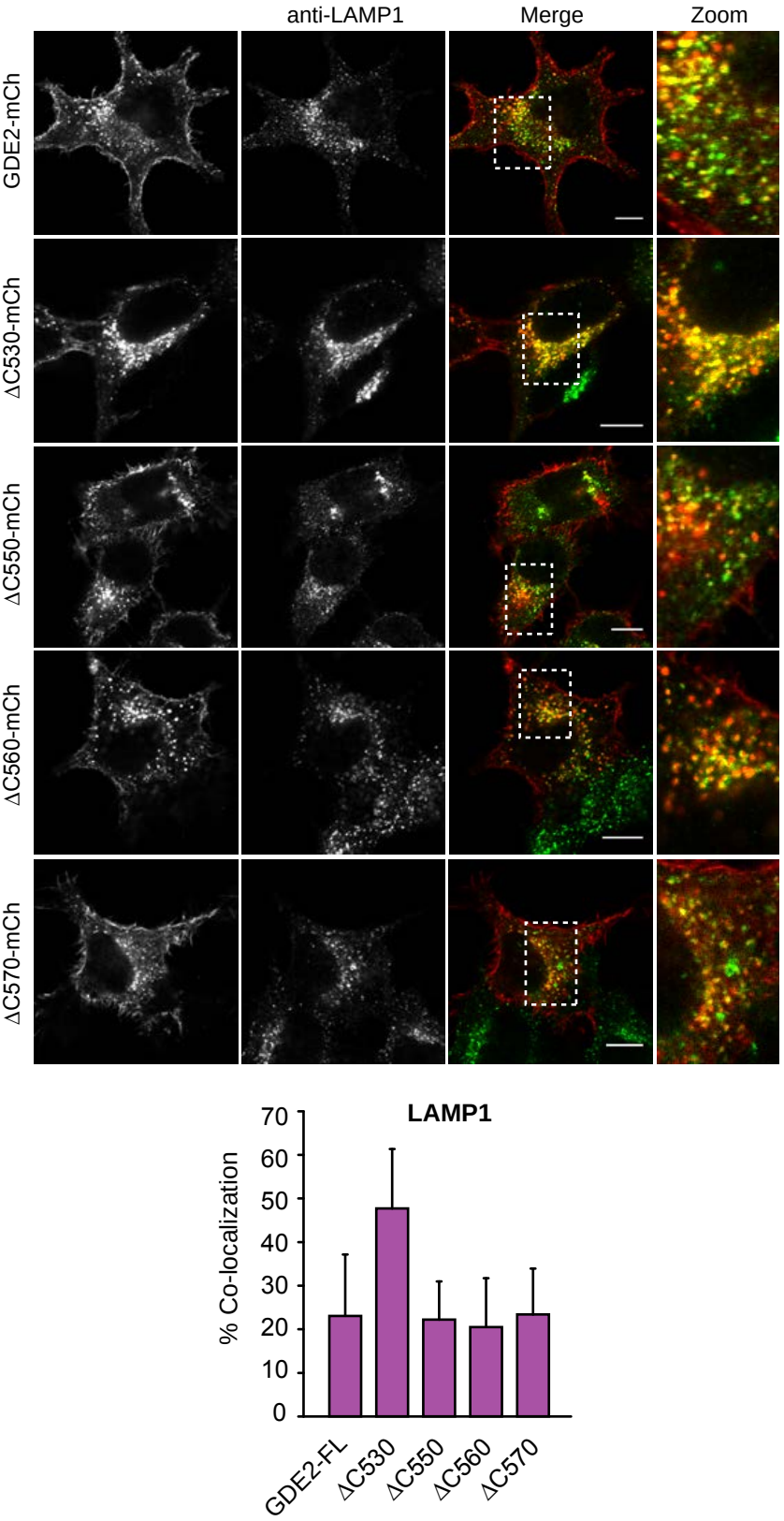

Figure S2. Lysosomal localization of GDE2 and its truncation mutants
N1E-115 cells expressing the indicated GDE2-mCh constructs were immunostained for LAMP1, using LAMP1-specific antibody. Bar, 10 μm. Lower panel, quantification of GDE2-LAMP1 co-localization.

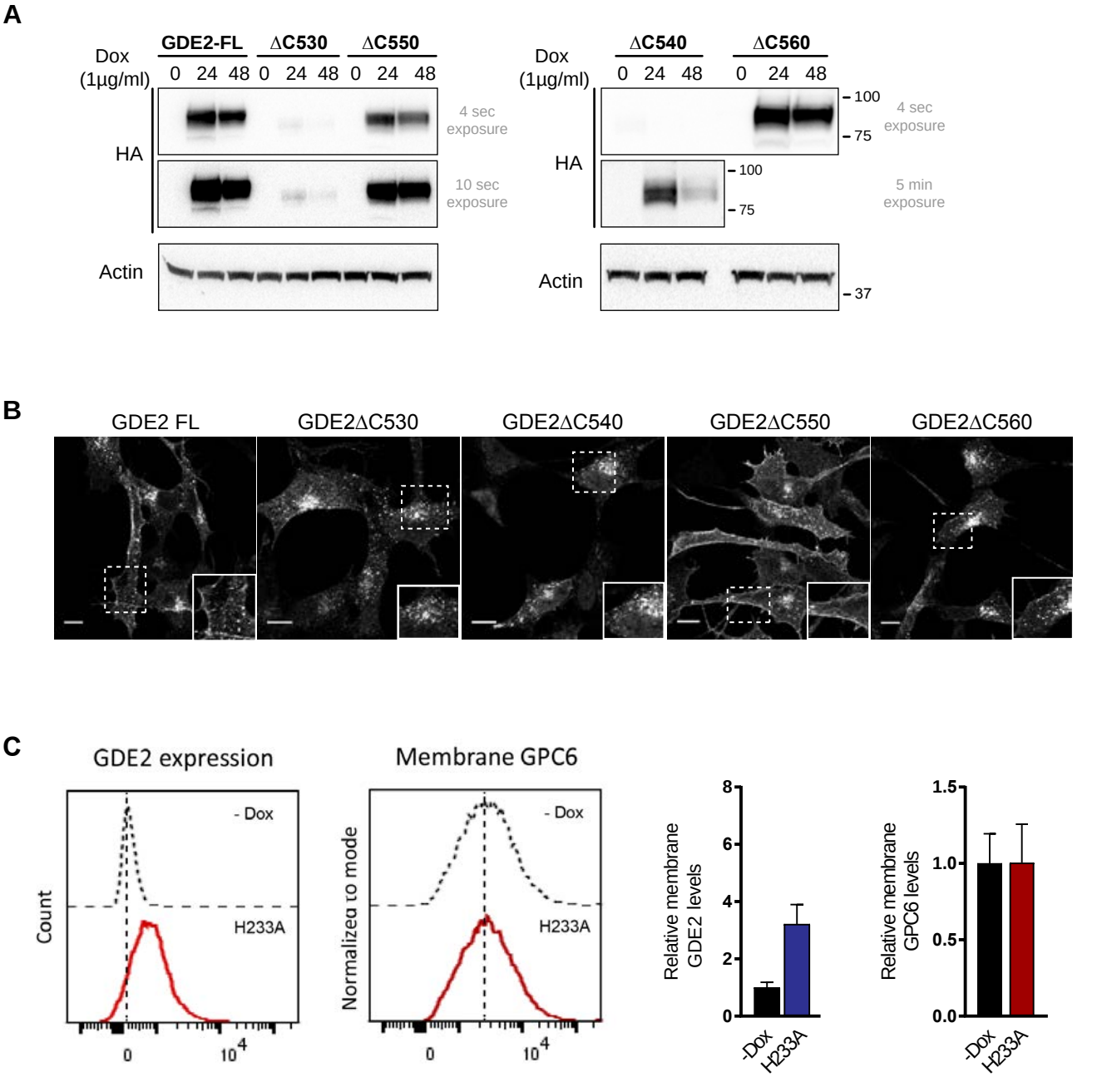

Figure S3. Expression and localization of GDE2 and truncation mutants in Dox-treated SH-SY5Ycells

A. Western blots showing expression of the indicated GDE2-HA constructs after 24 and 48 hrs of Dox treatment. Note differences in indicated exposure times. Actin was used as loading control. See also **Fig. 3A.**

B. Subcellular localization of the indicated GDE2 constructs. Bar, 10 µm. See also **Fig. 3B.**

C. Control experiment showing that GDE2(H233A) at the cell surface is inactive towards GPC6. Cell surface expressions were determined by FACS. See also Fig. 3D.